THE JOURNAL OF PHYSICAL CHEMISTRY B

Article

Photophysics of 2-(4'-amino-2'-hydroxyphenyl)-1*H*-imidazo-[4,5-c]Pyridine and Its Analogues: Intramolecular Proton Transfer Versus Intramolecular Charge Transfer

Santosh Kumar Behera, Ananda Karak, and Govindarajan Krishnamoorthy

J. Phys. Chem. B, **Just Accepted Manuscript** • DOI: 10.1021/jp5064808 • Publication Date (Web): 22 Oct 2014

Photophysics of 2-(4'-Amino-2'-hydroxyphenyl)-*1H*-imidazo-[4,5-c]pyridine and its analogues: Intramolecular Proton Transfer versus Intramolecular Charge Transfer

Santosh Kumar Behera, Ananda Karak and G. Krishnamoorthy*
Department of Chemistry
Indian Institute of Technology Guwahati
Guwahati 781039, India

Telephone: +91-361-2582315

E-mail: gkrishna@iitg.ernet.in

Abstract

Photophysical characteristics of 2-(4'-amino-2'-hydroxyphenyl)-*1H*-imidazo-[4,5-c]pyridine (AHPIP-c) have been studied in various aprotic and protic solvents using UV-Visible, steady state fluorescence and time-resolved fluorescence spectroscopic techniques. To comprehend the competition between the intramolecular charge transfer (ICT) and the excited state intramolecular proton transfer (ESIPT) processes, the photophysical properties of methoxy derivative 2-(4'-amino-2'-methoxyphenyl)-*1H*-imidazo-[4,5-c]pyridine (AMPIP-c) and 2-(4'-aminophenyl)-*1H*-imidazo-[4,5-c]pyridine (APIP-c) were also investigated. Though, APIP-c displays twisted ICT (TICT) emission in protic solvents AHPIP-c exhibits normal and tautomer emissions in aprotic as well as in protic solvents due to ESIPT. However, the methoxy derivative, AMPIP-c emits weak TICT fluorescence in methanol.

Keywords: TICT, ESIPT, proton coupled charge transfer, dual emission, hydrogen bond

1. Introduction:

Proton transfer and electron transfer are some of the important excited state phenomena those lead to dual emission.[1-11] These phenomena also play vital role in several photochemical and photobiological processes. In excited state intramolecular proton transfer (ESIPT) process, the photoinduced proton transfer from a protic acid group to a basic group occurs through an intramolecular hydrogen bond.[1-7] This results in a phototautomer in the excited state. On the other hand, in intramolecular charge transfer (ICT) process the charge is transfer from the charge donor to acceptor in the excited state that leads to formation of an ICT state.[8-11] Both ESIPT and ICT have diverse applications in numerous fields.[4,10-24] In addition, the coupled proton and charge transfer process is also observed in several systems.[25-31]

When groups responsible for ESIPT and ICT are combined in the same fluorophores then their photophysical properties become more interesting. Kasha *et al.* illustrated that the emission can occur from all three states of p-dimethylaminosalicylate, i.e. the locally excited state, the ICT state and the tautomer excited state and they compete with each other.[32-34] Conversely, in 4′-(*N*,*N*-diethylamino)-3-hydroxyflavone and its analogues emissions were observed only from the ICT and phototautomer states, and an equilibrium was established between the two states.[35-37] 7-*N*,*N*-Diethylamino-3-hydroxyflavone also emits only dual fluorescence and were observed from ICT and phototautomer states.[38,39] But there was a precursor–successor relationship between the two states. Recently, Guchhait *et al.* reported that the proton transfer supresses the ICT process in 4-(*N*,*N*-diethylamino)-2-hydroxybenzaldehyde.[40] In contrast, they illustrated that the proton transfer assists the charge transfer in some Schiff bases.[41] Rodríguez et al. revealed that 2-(4′-*N*,*N*-diethylamino-2′-hydroxyphenyl)benzimidazoles emit normal and tautomer emissions and no ICT emission.[42] However, they proposed ICT from the deprotonated dialkylaminophenol to the protonated

benzimidazole in the tautomeric form, but such an ICT process resulted in non-fluorescent tautomer. In flufenamic acid and mefenamic acid ESIPT occurs in nonpolar solvent and ICT fluorescence occurs in polar solvents.[43] A derivative of 9-aminoacridine exhibits a complex emission consist of normal emission, ICT emission and emission from the enol–imine tautomeric form.[44] p-*N*,*N*-Dimethylaminobenzoic acid emits only normal emission in nonpolar solvents but Yoon *et al.* found that p-*N*,*N*-dimethylaminosalicylic acid emits ICT emission in nonpolar solvents also.[45,46] Therefore, they proposed that the ESIPT through hydrogen bonding favoured the ICT process. Further they have demonstrated that when the intermolecular hydrogen bonding was supressed by complexation, the ICT emission enhanced due to intramolecular hydrogen bond that led to ESIPT. Similarly, though no ICT emission was detected from 4-aminobenzoic acid and ICT emission was reported from 4-aminosalicylic acid.

On the other hand, in 2-(4'-aminophenyl)-*1H*-imidazo[4,5-c]pyridine (APIP-c, Chart 1) intermolecular hydrogen bond promotes the formation of ICT emission.[47] Fasani *et al.* were the first one to observe ICT emission from APIP-c in protic solvent.[47] But they proposed that the hydrogen bonding of protic solvents with >NH and nitrogen of imdazole twist the acceptor (imidazopyridine) which results in a twisted ICT (TICT) state. Later studies from our group revealed that the hydrogen bonding of protic solvents with pyridyl nitrogen also plays a very crucial role in the formation of TICT state in 2-(4'-aminophenyl)imidazopyridines.[11,48-50] We also demonstrated that it is the dimethylamino group not the imidazopyridine ring that is twisted to form the TICT state.[11,48-50] The corresponding 2'-hydroxy analogue, 2-(2'-hydroxyphenyl)-*1H*-imidazo[4,5-c]pyridine (HPIP-c, Chart 1) also emits dual emission depending on the nature of the solvents.[51] But its' dual emission is due to formation of phototautomer by ESIPT process. The intensity ratio of tautomer emission to normal emission decreases with protic nature of the environment. Here,

we reported our investigation on 2-(4'-amino-2'-hydroxyphenyl)-*1H*-imidazo-[4,5-c]pyridine (AHPIP-c, Chart 1). So far, in the combined ESIPT-ICT system those reported in the literature, the intermolecular hydrogen bonding is not absolutely essential for ICT molecules to emit ICT emission.[32-46] AHPIP-c is the first molecule of this kind. The main objectives of the studies are to ascertain the roles of intermolecular hydrogen bond, intramolecular hydrogen bond and proton transfer in the ICT process and to find whether intramolecular hydrogen bond or proton transfer is competent to promote ICT. Further the studies in protic solvents will be more interesting to determine the dominating process (ICT or ESIPT) in protic solvent. For better understanding, we also studied the spectral characteristics of 2-(4'-amino-2'-methoxyphenyl)-*1H*-imidazo-[4,5-c]pyridine (AMPIP-c, Chart 1), APIP-c (Chart 1) and 2-phenyl-*1H*-imidazo-[4,5-c]pyridine (PIP-c, Chart 1).

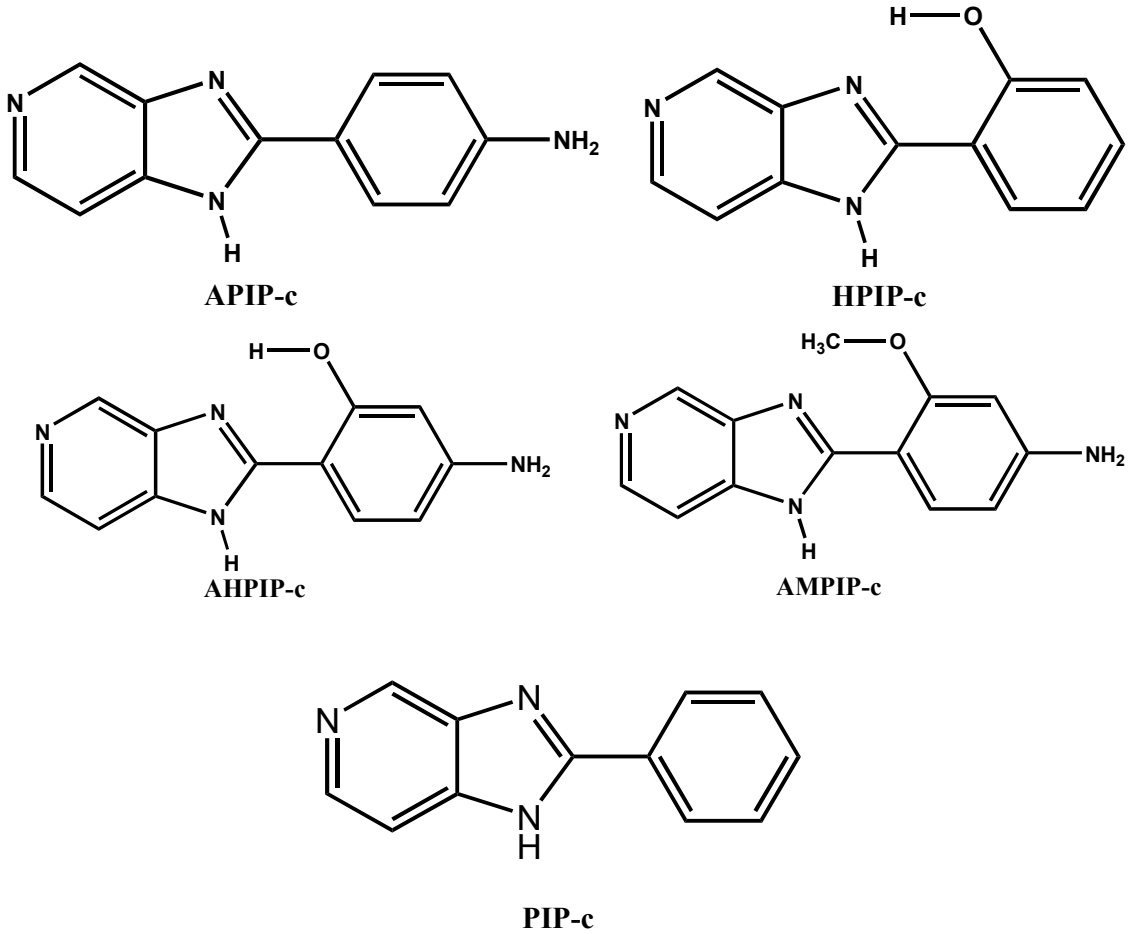

Chart 1. Structures of APIP-c, HPIP-c, AHPIP-c, AMPIP-c and PIP-c.

2. Materials and Methods

2.1 Synthesis

APIP-c, AHPIP-c and AMPIP-c were synthesized by refluxing 3,4-diaminopyridine and the corresponding 4-aminobenzoic acid in $POCl_3$ at 110°C by following the procedure for the synthesis of similar compounds.[52] After 8 hours the reaction mixtures were cooled to room temperature and poured into ice cold water. The solution was neutralized by concentrated sodium hydroxide solution. The precipitates were filtered and collected. The compounds were purified by column chromatography. The identities of the compounds were confirmed by NMR and HRMS mass data.

APIP-c

^{1}H NMR (400 MHz, DMSO-d_6): δ 12.83 (s, 1H), 8.76 (s, 1H), 8.20 (d, 1H), 7.95 (d, 1H), 7.87 (d, 2H), 6.67 (m, 2H), 5.72 (s, 2H).

^{13}C NMR (150 MHz, DMSO-d_6) δ 109.80, 112.45, 113.48, 116.17, 128.31, 129.55, 140.73, 151.30, 152.11, 171.95

ESI m/z $[M + H^+]$ = 211.097

AHPIP-c

^{1}H NMR (400 MHz, DMSO-d_6): δ 8.36 (s, 1H), 7.80 (s, 1H), 7.39 (t, 1H), 7.06 (d, 1H), 6.38 (d, 1H), 5.86 d, 1H), 4.9(br, 3H).

^{13}C NMR (150 MHz, DMSO-d_6) δ 99.44, 106.16, 106.77, 109.78, 111.49, 120.56, 130.72, 132.53, 137.97, 148.83, 155.20, 163.05

ESI m/z $[M + H^+]$: 227.095

AMPIP-c

^{1}H NMR (400 MHz, DMSO-d_6): δ 12.04 (s, 1H), 8.79 (s, 1H), 8.22 (d, 1H), 8.03 (d, 1H), 7.48 (d, 1H), 6.30 (m, 2H), 5.86 (s, 2H), 3.39 (s,3H)

^{13}C NMR (150 MHz, DMSO-d_6) δ 55.86, 96.64, 106.99, 108.32,112.30, 130.19, 140.50, 140.90, 143.04, 151.48, 153.13, 154.25, 158.86

ESI m/z [M + H^+] = 241.108

PIP-c is synthesized by heating 3,4-diaminopyridine and benzoic acid in polyphosphoric acid heated at 190°C for 5 h. The reaction mixture was cooled to room temperature and poured to ice cold water. The mixture was neutralized by KOH solution. The solid product thus obtained was dried in a desiccator. The dried solid product was recrystallized twice in methanol. The identity of the product was confirmed by NMR and HRMS mass data.

^{1}H NMR (600 MHz, $CDCl_3$): δ 8.86 (1H, s), 8.22 (1H, d), 8.08 (2H, dd), 7.36 (4H, m).

^{13}C NMR (150 MHz, $CDCl_3$): δ141.28, 130.52, 129.54, 128.81, 127.1

ESI m/z [M+H^+] 196.087

2.2. Spectral Measurements

All the spectral measurements were carried out with ~ 1 μM of solute in order to avoid aggregation and self-quenching. The absorption spectra were recorded by using Perkin Elmer Lambda 25 UV-Visible spectrophotometer. Steady state emission spectra were recorded on a HORIBA Jobin Yvon Fluorolog-3 fluorimeter. Fluorescence lifetimes were measured using time correlated single-photon counting (TCSPC) method on an Edinburgh Instrument Life-Spec II instrument. 308 nm LED or 375 nm laser diodes was used as the excitation source. The fluorescence decays were analysed by reconvolution method using the FAST software provided by Edinburgh Instruments. The goodness of fit was determined by the reduced χ^2 values and weighted residuals which were between the ranges of ± 4.

3. Results and discussion

3.1. 2-(4'-aminophenyl)-*1H*-imidazo[4,5-c]pyridine (APIP-c)

Fasani *et al.* studied only the steady state spectral characteristics of APIP-c in few selected solvents.[47] For a better comparative study we measured the steady state spectral characteristics of APIP-c in more solvents. The data are presented in Table 1 and the fluorescence spectra in few solvents are depicted in Figure 1. APIP-c exhibits only normal emission in aprotic solvents. In methanol TICT emission is observed at longer wavelength. Our results are in good agreement with the spectral maxima reported by Fasani *et al.* We measured the fluorescence spectra of APIP-c in more protic solvents. In all these solvents though no clear band appears (as in methanol), but long tailings are observed. We also carried out time resolved fluorescence measurements (Table 2). The fluorescence decay in propanol is shown as representative plot (Figure 2). Single exponential decays are detected when monitored at 380 nm, in all aprotic as well as protic solvents except in methanol. However, when monitored at 460 nm, biexponential decay was observed in all the protic solvents. The short lifetimes match with the lifetimes obtained at shorter wavelength. Therefore they can be assigned to normal emission. The long lifetime components are due to TICT emission and their relative amplitude increases with protic nature of the solvents. Thus, not only methanol but also other protic solvents induce the TICT emission in APIP-c. The absence of dual emission in aprotic solvent and its' presence in protic solvents may be due to enhancement in the electron withdrawing capacity of the acceptor by hydrogen bonding with protic solvents. Herbich *et al*. demonstrated that such an increase in the electron affinity by hydrogen bonding lowers the energy of the TICT state and the barrier for its' formation in 4-(*N*,*N*-dimethylamino)pyrimidines.[53]

The electronic transition dipole moment (M_{flu}) for the charge transfer state can be determined using following expression, [54]

$$k_f = \frac{64\pi^4}{3h}(n\bar{\nu}_{flu}^{TICT})^3 \left|M_{flu}\right|^2 \quad (1)$$

where k_f is the radiative rate constant, h is the Planck's constant and n is the refractive index. Since clear dual emission is observed only in methanol calculation of quantum yield is more reliable in methanol. Therefore, the M_{flu} is estimated in methanol. The quatum yield, radiative rate constant, nonradiative rate constant and electronic transition dipole moment for the longer wavelength emission are 0.039, 1.8 X 10^7 s^{-1}, 4.4 X 10^8 s^{-1} and 1.5 D, respectively. The small value of the electronic transition dipole moment determined for the longer wavelength emission suggest a small overlap between the donor and the acceptor orbitals. This supports the TICT model.[55-57] The absence of dual emission from PIP-c (the molecule which do not have electron donating amino group) in protic solvent and its enhancement in dimethylamino derivative of APIP-c further substantiates the TICT model (see later).

3.2. 2-(4'-amino-2'-hydroxyphenyl)-*1H*-imidazo[4,5-c] pyridine (AHPIP-c)

The absorption spectra of AHPIP-c were recorded in different solvents and the data are compiled in Table 3. Absorption spectra in all the solvents consist of one band at ~ 300 nm and another band at ~ 345 nm. The longer wavelength absorption band maxima of AHPIP-c are red shifted compared to those of APIP-c and HPIP-c. This is may be due to greater conjugation in AHPIP-c which has both hydroxyl and amino groups. Upon increasing the polarity and hydrogen bonding capacity of the solvents a small blue shift is observed in the longer wavelength absorption band maxima. Whereas, such a change produces a red shift in the absorption spectrum of APIP-c (Table 1) and a blue shift in the absorption spectrum of HPIP-c.[51]

Fluorescence spectral data of AHPIP-c in different solvents are compiled in Table 3. Figure 3 shows the representative spectra of AHPIP-c in selected solvents. Unlike APIP-c, in

AHPIP-c dual emission is observed in both aprotic and protic solvents. The fluorescence decays were monitored at both bands and were found to be single exponentials (Table 4). The fluorescence lifetime of the shorter wavelength emitting species is shorter than that of the longer wavelength emitting species.

Dogra *et al*. established HPIP-c exists in both *cis* and *trans* enol forms.[51] *Cis* enol upon excitation undergoes ESIPT to form a keto tautomer and the emission occurs from the tautomer, whereas the *trans*-enol upon excitation emits the normal emission. The shorter and the longer wavelength emissions were assigned to normal emission (from *trans* enol) and tautomer emission (from the tautomer formed by ESIPT from *cis*-enol), respectively. In APIP-c only a single emission is observed in aprotic solvents. But, Yoon *et al.* hypothesized that the activation energy for the ICT processes is lowered by the ESIPT through the intramolecular hydrogen bonding in 4-aminosalicylic acid.[45] Park *et al.* also described a consecutive ESIPT/ICT process that led to dual emission when different acceptors were substituted in the ESIPT exhibiting 2-(2'-hydroxyphenyl)benoxzazole.[58,59]

ESIPT yields a phototautomer whose dipole moment is lesser than the ground state. Therefore, upon increasing the polarity of the solvent, the excited state is less stabilized than the ground state. This lead to increase in the energy gap between the states, thus, a negative solvatochromism is experienced. On the other hand, ICT in the excited state generates a highly polar TICT state whose dipole moment is much higher than the ground state.[8-11] Consequently, the excited state is more stabilized with increase in environmental polarity which decreases the energy gap. Accordingly, it produces a red shift in the fluorescence spectra upon increasing the polarity of the environment. In AHPIP-c the longer wavelength emission is blue shifted with increase in solvent polarity (Table 3). In other words a negative solvatochromism is observed (Figure 4). Hence, it can be concluded that the longer wavelength emission of AHPIP-c in aprotic solvents is due to ESIPT. Guchhait *et al*. found

that in some Schiff bases the proton transfer assist the TICT process.[41] It was also reported that the ICT emission is at shorter wavelength than the tautomer emission. But the solvatochromic shift of the shorter wavelength emission is small to assign the shorter wavelength as TICT band. In addition the shorter wavelength band is blue shifted with respect to the TICT emission of APIP-c (Table 1 and 3). Therefore, the shorter wavelength and the longer wavelength emission from AHPIP-c in aproic solvents can be assigned to normal and tautomer emissions, respectively. This conclusion is further substantiated from the single emission observed in aprotic solvents from the methoxy derivative of AHPIP-c (see later).

TICT process is responsible for the longer wavelength emission of the 4-aminophenyl derivatives of imidazopyridines in protic solvents.[11, 47-50] But, in protic solvents also the longer wavelength emission of 2-hydroxyphenyl derivative is due to ESIPT process.[51] Protic solvents break the intramolecular hydrogen bond in *cis* enol which is perquisite for the ESIPT process. This decreases the tautomer intensity. In contrast, the intermolecular hydrogen bond with the charge acceptor favours the formation of ICT state thereby enhances the ICT emission.[11,47-50] Therefore, the effect of protic solvents is further more exciting. The single exponential decays of both emissions clearly suggest that in protic solvents also AHPIP-c exhibits only dual fluorescence and not the triple fluorescence. Therefore, it is clear that one of the processes (TICT or ESIPT) is supressed by the other in AHPIP-c. The longer wavelength fluorescence of AHPIP-c may be due to ESIPT or ICT process. The longer wavelength emission band maxima in protic solvents also show negative solvatochromism (Figure 4). The longer wavelength band maxima in methanol is blue shifted compared to nonpolar solvents (Table 3). This indicates that the longer wavelength emission is the tautomer emission. The intermolecular hydrogen bonding is essential for APIP-c to exhibit the TICT emission. In AHPIP-c, the ESIPT process completely prevents the ICT process in

protic solvents also despite fact that the protic solvents favour the intermolecular hydrogen bonding. In 4-(diethylamino)-2-hydroxybenzaldehyde also the TICT process is supressed by ESIPT process.[40] But the nature of 4-(diethylamino)benzaldehyde is different unlike in APIP-c, the protic environment is not essential for 4-(diethylamino)benzaldehyde to emit TICT emission. Rodríguez *et al.* illustrated though non emissive ICT is observed in 2-(4′-*N*,*N*-diethylamino-2′-hydroxyphenyl)benzimidazoles no ICT emission is found in aprotic or protic solvents.[42] But unlike AHPIP-c derivatives, 2-(4′-*N*,*N*-diethylamino-2′-hydroxyphenyl)benzimidazoles do not have pyridyl nitrogen which plays a crucial role in the hydrogen bonding induced TICT emission of 2-(4'-aminophenyl)imidazopyridines.[11,47-50] In AHPIP-c despite the presence of pyridyl nitrogen TICT emission is suppressed by ESIPT.

The fluorescence excitation spectra of AHPIP-c monitored at both emission maxima are different (Figure 5). This suggests that the ground state precursors for both the emissions are different. As mentioned earlier, HPIP-c and related molecules exist as *cis*-enol and *trans*-enol conformers. Accordingly, in AHPIP-c also the two different ground state species can be assigned *cis*- and *trans*- enols (Chart 2). Subsequently, two different lifetimes obtained for the normal and the tautomer emissions can be assigned to the lifetime of the excited *trans*-enol and the tautomer, respectively. The fluorescence lifetimes of both species of AHPIP-c are longer than those of respective forms of HPIP-c.[51] Such enhancements in radiative lifetimes are observed in ESIPT molecules also upon increasing conjugation.[41,51] The increase in polarity and hydrogen bonding capacity of the environment shifts the *cis*-enol-*trans*-enol equilibrium towards *trans*-enol. Therefore, the intensity ratio of the tautomer emission to normal emission decreases with increase in polarity and hydrogen bonding capacity of the solvent (Figure 6). The ratio is less in protic solvents than in aprotic solvents and, it decreases with the protic nature of the solvent. As the intermolecular hydrogen bond breaks the intramolecular hydrogen bond in *cis*-enol, the competition between the intramolecular and

intermolecular hydrogen bond decreases the relative population of *cis*-enol in protic solvents.[51] In other words, the ESIPT process is hindered by intermolecular hydrogen bonding and it is evident from Figure 6.

3.3. 2-(4′-amino-2′-methoxyphenyl)-*1H*-imidazo[4,5-c]pyridine (AMPIP-c)

To understand the role of ESIPT in supressing the ICT process of AHPIP-c, we further investigated the spectral properties of methoxy derivative AMPIP-c (Chart 1). Upon enhancing the polarity and the hydrogen bonding capacity of the solvents, though, little smaller than APIP-c a bathochromic shift is observed in the absorption spectrum of AMPIP-c (Table 5). This behaviour of AMPIP-c is different from that of methoxy derivative of HPIP-c. Dogra *et al.* reported that the absorption maxima of 2-(2'-methoxyphenyl)-1*H*-imidazo[4,5-c]pyridine (MPIP-c) are nearly insensitive to nature of the solvents.[60] Therefore, it is clear that the substitution of electron donating amino group make it sensitive to environment and characteristics of AMPIP-c are more closer to APIP-c than those of MPIP-c.

The fluorescence maxima of AMPIP-c are also more sensitive to the solvent polarity (Figure 7 and Table 5). Same as in APIP-c a positive solvatochromism is observed. But the charge transfer is less in AMPIP-c than in APIP-c. This is substantiated by the lower dipole moment of AMPIP-c than APIP-c (see later). The TICT emission of AMPIP-c is not as prominent as in APIP-c only long tail is found in methanol (Figure 1 and Figure 7). The excited decays of AMPIP-c measured in all solvents except methanol are single exponentials (Table 6). Attempt to fit the single exponential decay to the fluorescence decay in methanol resulted in poor fit with high chi square (χ^2). But the biexponential fit yields good results with two different lifetimes which further substantiate the presence of two different emitting species (Figure 8 and Table 6). By analogy with APIP-c they may be assigned to normal and TICT emitting species. In other protic solvents even when monitored at 465 nm single

exponential decays are found (Supporting Information, Table S1). The fluorescence lifetime also matches with the fluorescence lifetime obtained by monitoring at 385 nm. This shows that except methanol other alcohols do not induce TICT emission in AMPIP-c. Therefore, it is clear that the methoxy substitution at ortho position weaken the TICT emission of AMPIP-c. Like AHPIP-c, 2-(4′-*N*,*N*-diethylamino-2′-hydroxyphenyl)benzimidazoles also undergo ESIPT and no ICT emission was observed. But unlike AMPIP-c, the methoxyderivative derivative of 2-(4′-*N*,*N*-diethylamino-2′-hydroxyphenyl)benzimidazoles did not exhibit even weak TICT emission.

3.4 Solvatochromismic approach

Lippert-Mataga analysis[61] is employed to estimate the excited state dipole moments of the molecules to verify the charge transfer characteristics in the excited state.

$$\bar{\nu}_{ss} = \left[\frac{2(\mu_e - \mu_g)^2}{hca^3}\right]\Delta f + \text{Constant} \qquad (2)$$

Where $\bar{\nu}_{ss}$ is the Stokes shift, μ_e and μ_g are the excited state and ground state dipole moments of the molecule and *a* denotes the Onsagar cavity radius. The orientation polarizability is defend by

$$\Delta f = \left[\frac{\varepsilon - 1}{2\varepsilon + 1} - \frac{n^2 - 1}{2n + 1}\right] \qquad (3)$$

Where ε and n are the dielectric constant and refractive index of the solvents respectively, The Lippert-Mataga plot is constructed for normal emissions of APIP-c, AMPIP-c and AHPIP-c (Figure 9). Using the Onsager radius and the ground state dipole moments obtained from the DFT calculations and the slope obtained from Lippert plot and, the excited state dipole moments are calculated. The excited state dipole moment, thus determined for APIP-c, AMPIP-c and AHPIP-c (*trans*-enol) are 11.9 D, 10.8 D and 10.8 D, respectively. The ground

state dipole moments of APIP-c, AMPIP-c and AHPIP-c (*trans*-enol) are 7.1 D, 7.8 D and 9.6 D, respectively. Thus, it can be interpreted that the charge transfer enhanced in the excited state. The enhancement in excited state charge transfer is more in APIP-c than in AMPIP-c, which is higher than that in AHPIP-c.

The dipole moments for the normal emissions suggest appreciable charge transfer from the donor to acceptor in all the molecules. Unfortunately, the longer wavelength emission is observed from AMPIP-c only in methanol. Even the longer wavelength emission of APIP-c is buried under the normal emission in other protic solvents expect methanol. Therefore estimating the dipole moment of the longer wavelength emitting state by solvatochromic approach is not viable. Hence, to substantiate that the longer wavelength emission is a TICT emission we synthesized the fluorophore without the charge donor (amino group). The spectral characteristics of PIP-c, thus synthesized are summarized in Table 7 and the fluorescence spectra are presented in Figure 10. Unlike in amino derivatives no dual emission is observed in PIP-c in not only in aprotic solvents but also in protic solvents. On the other hand, when the electron donating ability of the donor is higher the longer wavelength emission induced by protic solvents increases (in methanol the intensity ratio of longer wavelength to shorter wavelength is 0.18 for APIP-c and 0.30 for the dimethyl derivative of APIP-c, 2-(4'-dimethylaminophenyl)imidazo[4,5-c]pyridine).[48] The dependence of the longer wavelength emission with the capacity of charge donor is consistent with our assignment that the longer wavelength emission is the TICT emission. In APIP-c analogue, 2-(4'-dimethylaminophenyl)imidazo[4,5-b]pyridine also dual emission was observed only in protic solvents. Since 2-(4'-dimethylaminophenyl)imidazo[4,5-b]pyridine emits clear dual emission in other protic solvents also the dipole moment was estimated using longer wavelength emission by solvatochromic approach. The estimated dipole moments (μ_e = 12.0 D (normal) 24.6 D (TICT)) substantiated the assignment of the TICT mechanism.[48,62]

Kamlet Taft solvatochromic method is widely used to understand the interaction between the solute and solvent molecules.[63] This multi-parametric approach separates the effects of polarity and hydrogen bonding, and provides useful information. According to multiple linear regression analysis approach the spectral band energy (in cm^{-1})

$$\bar{\nu} = \bar{\nu}^{0} + s\pi^{*} + a\alpha + b\beta \qquad (4)$$

where π^*, α and β are the polarity/polarizability, hydrogen bond donating ability and hydrogen bond accepting capacity of the solvents, respectively. The sensitivity to each individual parameter were given as *s*, *a* and *b* coefficients. The fits obtained using the absorption spectral data are presented below:

$$\bar{\nu}\,(\text{APIP-c}) = 32589 - 863\pi^{*} - 750\alpha - 24\beta \ (r = 0.89) \qquad (5)$$

$$\bar{\nu}\,(\text{AHPIP-c}) = 28364 + 880\pi^{*} + 306\alpha - 57\beta \ (r = 0.93) \qquad (6)$$

$$\bar{\nu}\,(\text{AMPIP-c}) = 31205 - 1167\pi^{*} - 713\alpha - 260\beta \ (r = 0.89) \qquad (7)$$

The $\bar{\nu}^{0}$ values obtained in all the molecules are in good agreement with the values in nonpolar solvent. The negative and positive values of coefficients indicate the stabilization and destabilization of the system by individual parameter. Not only the polarity parameter but also the hydrogen bond donating ability of the solvent has positive coefficient for the hydroxyl derivative. The hydroxyl derivative has strong intramolecular hydrogen bond which stabilizes the system. Therefore, any intermolecular hydrogen bonding through solvents destabilizes it. On the other hand, when there was no intramolecular hydrogen bond the intermolecular hydrogen bond stabilizes the molecules. Therefore, the intermolecular hydrogen bonding stabilizes APIP-c and AMPIP-c. In other words, when the intramolecular hydrogen bonding that leads to ESIPT is prevented the intermolecular hydrogen bonding dominates and it allows TICT to prevail.

Less sensitivity of the fluorescence maxima toward the solvent results in a poor correlation for AHPIP-c. However, reasonably good correlations were obtained for APIP-c and AMPIP-c and are shown below:

$$\bar{\nu}\,(\text{APIP-c}) = 27514 - 1203\pi^* - 863\alpha - 243\beta \ (r = 0.82) \qquad (8)$$

$$\bar{\nu}\,(\text{AMPIP-c}) = 27982 - 1507\pi^* - 825\alpha - 552\beta \ (r = 0.91) \qquad (9)$$

Like the ground state, the excited state also stabilized by both polarity and hydrogen bonding parameters. The solvatochromic approach clearly shows that the intermolecular hydrogen bonding plays an important role in the stabilization of APIP-c and AMPIP-c. The ESIPT prevents the TICT processes of AHPIP-c in protic solvents also and blocking of ESIPT in AMPIP-c opens the TICT channel due to strong intermolecular hydrogen bonding.

3.5 Theoretical calculations

All the calculations were performed using Gaussian 09 program.[64] The ground state geometries were optimized DFT method. The first excited state geometries were optimized using *ab* initio configuration interaction singles (CIS) approach. The excitation and the emission energies were computed by TDDFT method from the optimized geometries as input (vertical transitions). Moderate to good correlations were obtained between the computed and the experimental transition energies (Table 8, 9 and 10). B3LYP function and 6-31G(d,p) basis sets were employed in the calculations. The integral equation formalism-polarizable continuum (IEF-PCM) model was used to include the solvent stabilization effects. The data computed for all the molecules in acetonitrile are compiled in Table 8 and the frontier molecular orbitals are given in the Supporting Information. Both *cis*- and *trans*- enol of AHPIP-c are included for the excitation energies comparison. Since in the excited state *cis*-enol undergoes ESIPT to form keto tautomer, the structure of the keto form is optimized in

the first excited state. The emission energy obtained for keto is compiled instead of *cis*-enol. The lowest energy transitions in all the molecule are single excitations from the highest occupied molecular orbital (HOMO) to the lowest unoccupied molecular orbital (LUMO). These transitions are strongly allowed as indicated by the higher oscillator strength and the first excited states are ππ* state. However, the S_0-S_2 and S_0-S_3 transitions involve multiple excitations and have smaller oscillator strength.

APIP-c and AMPIP-c emit both normal and TICT emissions in methanol. Therefore, we also computed the transitions for APIP-c and AMPIP-c in methanol (as solvent) for the methanol complexes of APIP-c and AMPIP-c. The methanol complex comprise of several methanol molecules forming hydrogen bond at different sites. Since, the hydrogen bonding at pyridyl nitrogen is more crucial for the formation of TICT state,[11,48-50] we have performed the calculations by adding single methanol at pyridyl nitrogen to save the computational time. We considered the twisting of both phenyl ring and amino group. The transitions of normal, phenyl twisted and amino twisted forms of APIP-c and AMPIP-c are presented in Table 9 and 10. The transition energies computed for the phenyl twisted forms are higher than the corresponding transition energies of the normal forms. Even the emission energies of the S_0-S_1 transition of the phenyl twisted rotamers are higher than the emission energies of the S_0-S_1 transition of the normal forms. Therefore, it is clear that TICT emission of APIP-c and AMPIP-c are not from the phenyl twisted forms. However, transition energies predicted for the amino twisted forms are less than the corresponding transition energies of the normal forms. The S_0-S_1 transitions are defined by HOMO-LUMO single excitation and the oscillator strengths of S_0-S_1 for the normal forms are higher which indicate that these transitions are allowed. In amino twisted form the first excited states are defined by multiple excitation. In both molecules the first excited states are formed by the excitations from HOMO to higher orbitals. The contribution of HOMO → LUMO and HOMO → LUMO + 3

are 0.68849 (87.2 %) and 0.10095 (12.8 %) respectively in APIP-c. In AMPIP-c, the contribution HOMO → LUMO, HOMO → LUMO + 1 and HOMO → LUMO + 3 are 0.67742 (71.7 %), 0.13649 (14.5 %) and 0.13077 (13.8 %) respectively. The charge is localized on the donor amino group in the HOMO and in the higher orbital it is localized on the rest of the molecule (Figure 11). Therefore, the transition from HOMO involves the charge transfer from amino groups to other part of the molecule and there is a minimum overlap between them. Further, negligible oscillator strengths for the transitions of amino twisted corroborate this. Thus, the result can be interpreted by TICT model. In LUMO + 1 and LUMO + 3 orbitals the charge density on the imidazole ring is less. The contributions of the excitations to those molecular orbitals are more in AMPIP-c than APIP-c. Incidentally, AMPIP-c, which emits relatively weaker TICT emission, the oscillator strength for the TICT emission though it is very little, it has non-zero value. However, the calculation predicts the oscillator strength for the TICT emission in APIP-c as zero.

The calculation predicted that the amino group is out of plane from the phenyl ring by nearly same angle (22°) in methanol complexes of both APIP-c and AMPIP-c. However, the imdazopydridine ring and the phenyl ring are out of plane by 4° and 38°, respectively in APIP-c and AMPIP-c complexes. In APIP-c and AMPIP-c the TICT state is formed by the twisting of the amino group. The twisting of phenyl ring is not a favoured process for formation of TICT state in AMPIP-c also. Therefore, we speculate that the nonplanar geometry between the phenyl ring and imdazopydridine ring in methoxy molecule may be responsible for its' weak TICT emission. Yoon *et al*. proposed that the planarization of the benzene ring with carboxylic acid group favours the TICT processes in dialkylamino benzoic acids owing to large charge flow from the phenyl ring to carboxylic acid.[65,66] The twisting of phenyl ring might have reduced the charge flow from the phenyl ring to imidazopyridine ring in AMPIP-

c. Other spectral characteristics also suggest that the intramolecular charge transfer is less in AMPIP-c than in APIP-c

4. Conclusion

APIP-c exhibits dual emission only in protic solvents. Dual fluorescence is observed from AHPIP-c in all solvents. The shorter wavelength emission is the normal emission from the excited *trans*-enol. Unlike in APIP-c the longer wavelength emission is the tautomer emission. Like in HPIP-c, the radiative lifetime of the tautomer emission is longer than normal emission. But the lifetime of both normal and tautomer emissions of AHPIP-c are longer than the respective lifetimes of HPIP-c. The intensity ratio of the tautomer emission to the normal emission is sensitive to nature of the solvent. Not only in aprotic solvents but also in protic solvents the ESIPT process supresses the TICT process. When the intramolecular hydrogen bond is blocked, the methoxy derivative of AHPIP-c, AMPIP-c emits normal emission in most of the solvent. But it exhibits the TICT emission in methanol. The TICT emission of AMPIP-c is weaker than the TICT emission of APIP-c. The substitution of bulky methoxy group twisted the imidazopyridine out of plane from the benzene ring and thereby reduced the ICT from the benzene ring to imidazopyridine ring. The amino group twist to form the emitting TICT state in both APIP-c and AMPIP-c. In the TICT geometry there is a minimum overlap between the amino group and rest of the molecule.

Acknowledgement

The authors thank Department of Science and Technology (DST), India for the financial support (SR/S1/PC/0046/2010) and the Central Instruments Facility (CIF), Indian Institute of Technology Guwahati for the LifeSpec II instrument and NMR spectrometers.

Supporting Information:

The fluorescence lifetime data of AMPIP-c in protic solvent (obtained by monitoring at 465 nm), full authors list for reference 64 and the computed frontier molecular orbitals. This information is available free of charge via the Internet at http://pubs.acs.org

References

1. Kasha, M. Proton –Transfer Spectroscopy – Perturbation of the Tautomerization Potential. *J. Chem. Soc., Faraday Trans. 2.* **1986**, *82*, 2379-2392.
2. Douhal, A.; Kim, S. K.; Zewail, A. H., Femtosecond Molecular-Dynamics of Tautomerization in Model Base-Pairs. *Nature*. **1995**, *378*, 260-263.
3. Kwon, J. E.; Park, S. Y. Advanced Organic Optoelectronic Materials: Harnessing Excited-State Intramolecular Proton Transfer (ESIPT) Process. *Adv. Mater.* **2011**, *23*, 3615-3642.
4. Zhao, J.; Ji, S.; Chen, Y.; Guo, H.; Yang, P. Excited State Intramolecular Proton Transfer (ESIPT): From Principal Photophysics to the Development of New Chromophores and Applications in Fluorescent Molecular Probes and Luminescent Materials. *Phys. Chem. Chem. Phys.* **2012**, *14*, 8803–8817.
5. Iyer, E. S. S.; Khorwal, V.; Sundararajan M.; Datta, A. Intense Phototautomer Emission of 2-(3'-pyridyl)benzimidazole Encapsulated in Nafion Membrane. *RSC. Adv.* **2013**, *3*, 1145-1150.
6. Vetokhina, V.; Dobek, K.; Kijak, M.; Kaminska, I. I. ; Muller, K. ; Thiel, W. R. ; Waluk, J.; Herbich, J. Three Modes of Proton Transfer in One Chromophore: Photoinduced Tautomerization in 2-(1H-Pyrazol-5-yl)Pyridines, Their Dimers and Alcohol Complexes. *Chemphyschem*, **2012**, *13*, 3661-3671.

7. Basaric, N.; Doslic, N.; Ivkovic, J. ; Wang, Y. –H. ; Veljkovic, J.; Mlinaric-Majerski, K.; Wan, P. Excited State Intramolecular Proton Transfer (ESIPT) from Phenol to Carbon in Selected Phenylnaphthols and Naphthylphenols. *J. Org. Chem*. **2013**, *78*, 1811-1823.
8. Grabowski, Z. R.; Rotkiewicz, K.; Rettig, W. Structural Changes Accompanying Intramolecular Electron Transfer: Focus on Twisted Intramolecular Charge-Transfer States and Structures. *Chem. Rev.* **2003**, *103*, 3899-4031.
9. Rettig, W. Charge Separation in Excited States of Decoupled Systems-TICT Compounds and Implications Regarding the Development of New Laser Dyes and the Primary Process of Visionand Photosynthesis. *Angew. Chem., Int. Ed. Engl.***1986**, *25*, 971-988.
10. Herbich, J.; Kapturkiewicz, A. Electronic Structure and Molecular Conformation in the Excited Charge Transfer Singlet-States of 9-Acridyl and Other Aryl Derivatives of Aromatic Amines. *J. Am. Chem. Soc.* **1998**, *120*, 1014-1029.
11. Chipem, F. A. S.; Mishra, A.; Krishnamoorthy, G. The Role of Hydrogen Bonding in Excited State Intramolecular Charge Transfer. *Phys. Chem. Chem. Phys.* **2012**, *14*, 8775-8790.
12. Sakai, K.; Tsuzuki, T.; Itoh, Y.; Ichikawa, M.; Taniguchi, Y. Using Proton-Transfer Laser Dyes for Organic Laser Diodes. *Appl. Phys. Lett*. **2005**, *86*, 081103.
13. Fluegge, A. P.; Waiblinger, F.; Stein, M.; Keck, J.; Kramer, H. E.A.; Fischer, P.; Wood, M. G.; DeBellis, A. D.; Ravichandran, R.;Leppard, D. Probing the Intramolecular Hydrogen Bond of 2-(2-hydroxyphenyl)benzotriazoles in Polar Environment: A Photophysical Study of UV Absorber Efficiency. *J. Phys. Chem. A* **2007**, *111*, 9733−9744.

14. Wu, J.; Liu, W.; Ge, J.; Zhang, H.; Wang, P. New Sensing Mechanisms for Design of Fluorescent Chemosensors Emerging in Recent Years. *Chem. Soc. Rev*. **2011**, *40*, 3483−3495.

15. Chipem, F. A. S.; Behera, S. K.; Krishnamoorthy, G. Ratiometric Fluorescence Sensing Ability of 2-(2′-hydroxyphenyl)benzimidazole and Its Nitrogen Substituted Analogues Towards Metal Ions. *Sens. Actuators B: Chem.***2014**, *191*, 727-733.

16. Lim, S. J.; Seo, J.; Park, S. Y. J. Photochromic Switching of Excited-state Intramolecular Proton-Transfer (ESIPT) Fluorescence: A Unique Route to High-contrast Memory Switching and Nondestructive readout. *J. Am. Chem. Soc.* **2006**, *128*, 14542−14547.

17. Mutai, T.; Tomoda, H.; Ohkawa, T.; Yabe, Y.; Araki, K. Switching of Polymorph-Dependent ESIPT Luminescence of an Imidazo[1,2-a]pyridine Derivative. *Angew.Chem., Int. Ed.* **2008**, *47*, 9522−9524.

18. Lapinski, L.; Nowak, M. J.; Nowacki, J.; Rode, M. F.;Sobolewski, A. L. A Bistable Molecular Switch Driven by Photoinduced Hydrogen-Atom Transfer. *ChemPhysChem*. **2009**, *10*, 2290−2295.

19. Park, S.; Seo, J.; Kim, S. H.; Park, S. Y. Tetraphenylimidazole-based Excited-state Intramolecular Proton-transfer Molecules for Highly Efficient Blue Electroluminescence. *Adv. Funct. Mater*. **2008**, *18*, 726−731.

20. Klymchenko, A. S.; Demchenko, A. P. Electrochromic Modulation of Excited-state Intramolecular Proton Transfer: The New Principle in Design of Fluorescence Sensors. *J. Am. Chem. Soc.* **2002**, *124*, 12372-12379.

21. Pivovarenko, V. G.; Vadzyuk, O. B.; Kosterin, S. O. Fluorometric Detection of Adenosine Triphosphate with 3-Hydroxy-4′-(dimethylamino)flavone in Aqueous Solutions. *J. Fluoresc.* **2006**, *16*, 9-15.

22. Henary, M. M.; Wu, Y.; Fahrni, C. J. Zinc(II)-selective Ratiometric Fluorescent Sensors Based on Inhibition of Excited-State Intramolecular Proton Transfer. *Chem. Eur. J.* **2004**, *10*, 3015-3025.

23. Lin, Q.; Liu, X.; Wei, T. –B.; Zhang, Y.–M. TICT-ICT State Change Mechanism Based Acetate Fluorescent Sensor Act as an "Off-On-Off" Switch and Logic Gate. *Sens. Actuators B: Chem.* **2014**, *190*, 459-463.

24. Mahato, P. ; Saha, S. ; Das, A. Rare Example of TICT Based Optical Responses for the Specific Recognition of Cr3+ by a 2,2':6 ',2 "-Terpyridine Derivative and Demonstration of Multiple Logic Operations. *J. Phys. Chem. C* **2012**, 116, 17448-17457.

25. Chou, P.-T.; Yu, W.-S.; Cheng, Y.-M.; Pu, S.-C.; Yu, Y.-C.; Lin,Y.-C.; Huang; Chen, C.-T. Solvent-Polarity Tuning Excited-State Charge Coupled Proton-Transfer Reaction in p-*N*,*N*-Ditolylaminosalicylaldehydes. *J. Phys. Chem. A* **2004**, *108*, 6487−6498.

26. Zgierski, M. Z.; Fujiwara, T.; Lim, E. C. Coupled Electron and Proton Transfer Processes in 4-Dimethylamino-2-hydroxy-benzaldehyde. *J. Phys. Chem. A* **2011**, *115*, 10009−10017.

27. Brenlla, A.; Rodríguez-Prieto, F.; Mosquera, M.; Ríos, M. A.; Ríos Rodríguez, M. C. Solvent-Modulated Ground-State Rotamerism and Tautomerism and Excited-State Proton-Transfer Processes in o-Hydroxynaphthylbenzimidazoles. *J. Phys. Chem. A* **2008**, *113*, 56−6.

28. Hsieh, C. C.; Jiang, C. M.; Chou, P. T. Recent Experimental Advances on Excited-State Intramolecular Proton Coupled Electron Transfer Reaction. *Acc. Chem. Res*. **2010**, *43*, 1364−1374.

29. Hammes-Schiffer, S.; Stuchebrukhov, A. A. Theory of Coupled Electron and Proton Transfer Reactions. *Chem. Rev*. **2010**, *110*, 6939−6960.

30. Weinberg, D. R.; Gagliardi, C. J.; Hull, J. F.; Murphy, C. F.;Kent, C. A.; Westlake, B. C.; Paul, A.; Ess, D. H.; McCafferty, D. G.; Meyer, T. J. Proton-Coupled Electron Transfer. *Chem. Rev.* **2012**, *112*, 4016−4093.

31. Ghosh, R.; Palit, D. K. Dynamics of Solvent Controlled Excited State Intramolecular Proton Transfer Coupled Charge Transfer Reactions. *Photochem. Photobiol. Sci.*, **2013**, *12*, 987-995.

32. Gormin, D.; Kasha, M. Triple Fluorescence in Aminosalicylates-Modulation of Normal, Proton-Transfer, and Twisted Intramolecular Charge – Transfer (TICT) Fluorescence by Physical and Chemical Perturbation. *Chem. Phys. Lett*. **1988**, 153, 574–576.

33. Gormin D.; Kasha, M. A Comparative Picosecond Spectroscopic Study of the Competitive Triple Fluorescence of Aminosalicylates and Benzanilides. *Chem. Phys*. **1989**, *136,* 321–334.

34. Gormin, D.; Heldt, J.; Kasha, M. Molecular Phosphorescence Enhancement via Tuning Through Proton Transfer Potentials. *J. Phys. Chem.* **1990**, *94*, 1185–1189.

35. Chou, P. T.; Martinez, M. L.; Clements, J. H. J. Reversal of Excitation Behaviour of Proton-Transfer Vs Charge-Transfer by Dielectric Perturbation of Electronic Manifolds. *J. Phys. Chem*. **1993**, *97*, 2618–2622.

36. Chou, P. T.; Martinez, M. L.; Clements, J. H. The Observation of Solvent –Dependent Proton –Transfer Charge Transfer Lasers From 4′-Diethylamino-3-hydroxyflavon. *Chem. Phys. Lett.* **1993**, *204*, 395–399.

37. Parsapour, F.; Kelley, D. F. Torsional and Proton Transfer Dynamics in Substituted 3-Hydroxyflavones. *J. Phys. Chem.* **1996**, *100*, 2791–2798.

38. Chou, P.-T.; Huang, C.; Pu, S.-C.; Cheng, Y.-M.; Liu, Y.-H.; Wang, Y.; Chen, C.-T. Tuning Excited-State Charge/Proton Transfer Coupled Reaction via the Dipolar Functionality. *J. Phys. Chem. A*. **2004**, *108*, 6452–6454.

39. Cheng, Y.-M. ; Pu, S.-C. ; Yu, Y.-C. ; Chou, P.-T. ; Huang, C.-H. ; Chen, C.-T. ; Li, T.-H. ; Hu, W.-P. Spectroscopy and Dynamics of 7-*N,N*-diethylamino-3-hydroxyflavone. The Correlation of Dipole Moments Among Various States to Rationalize the Excited-State Proton Transfer Reaction. *J. Phys. Chem. A*. **2005**, *109*, 11696–11706.

40. Jana, S.; Dalapati, S.; Guchhait, N. Excited State Intramolecular Charge Transfer Suppressed Proton Transfer Process in 4‑(Diethylamino)-2-hydroxybenzaldehyde. *J. Phys. Chem. A* **2013**, *117*, 4367−4376.

41. Jana, S.; Dalapati, S.; Guchhait, N. Proton Transfer Assisted Charge Transfer Phenomena in Photochromic Schiff Bases and Effect of –NEt_2 Groups to the Anil Schiff Bases. *J. Phys. Chem. A* **2012**, *116*, 10948−10958.

42. Ríos Va´zquez, S.; Ríos Rodríguez, M. C.; Mosquera, M.; Rodríguez-Prieto, F. Rotamerism, Tautomerism, and Excited-State Intramolecular Proton Transfer in 2-(4′-N,N-Diethylamino-2′-hydroxyphenyl)benzimidazoles: Novel Benzimidazoles Undergoing Excited-State Intramolecular Coupled Proton and Charge Transfer. *J. Phys. Chem. A* **2008**, *112*, 376-387.

43. El-Kemary, M. A. Relaxation Pathways of Photoexcited Non-steroidal Anti-inflammatory Drugs: Flufenamic and Mefenamic acid. *Chem. Phys.* **2003**, *295*, 1–10.

44. Pereira, R. V.; Ferreira, A. P. G.; Gehlen, M. H. Excited-State Intramolecular Charge transfer in 9-Aminoacridine Derivative. *J. Phys. Chem. A*. **2005**, *109*, 5978–5983.

45. Kim, Y.; Yoon, M.; Kim, D. Excited-State Intramolecular Proton Transfer Coupled-Charge Transfer of p-*N*, *N*-dimethylaminosalicylic Acid in Aqueous beta-Cyclodextrin Solutions. *J. Photochem. Photobiol., A*. **2001**, *138*, 167–175.

46. Kim, Y.; Yoon, M. Intramolecular Hydrogen Bonding Effect on the Excited-State Intramolecular Charge Transfer of p-Aminosalicylic Acid. *Bull. Korean Chem. Soc.* **1998**, *19*, 980–985.

47. Fasani, E.; Albini, A.; Savarino, P.; Viscardi, G.; Barni, E. The Role of Hydrogen Bonding in Excited State Intramolecular Charge Transfer Hydrogen Bonding, Protonation and Twisting in the Singlet Excited State of some 2-(4-Aminophenyl)pyrido-oxa-, -thia-, and –imidazoles. *J. heterocyclic chem.* **1993**, *30*, 1041-4044.

48. Krishnamoorthy, G.; Dogra, S. K. Dual Fluorescence of 2-(4'-*N,N*-Dimethylaminophenyl)pyrido[3,4-d]imidazole: Effect of Solvents. *Spectrochim. Acta, A.* **1999**, *55*, 2647-2658.

49. Dash, N.; Chipem, F. A. S.; Swaminathan, R.; Krishnamoorthy, G. Hydrogen Bond Induced Twisted Intramolecular Charge Transfer in 2-(4′-*N*,*N*-dimethylaminophenyl)imidazo[4,5-b]pyridine. *Chem. Phys. Lett.* **2008**, *460*, 119-124.

50. Mishra, A.; Sahu, S.; Dash, N.; Behera, S. K.; Krishnamoorthy, G. Double Proton Transfer Induced Twisted Intramolecular Charge Transfer Emission in 2‑(4′‑*N*,*N*‑Dimethylaminophenyl)imidazo[4,5-b]pyridine. *J. Phys. Chem. B* **2013**, *117*, 9469−9477

51. Balamurali, S. S.; Dogra, S. K. Excited State Intramolecular Proton Transfer in 2-(2'-hydroxyphenyl)-1H-imidazo[4,5-c]pyridine: Effects of Solvent. *J. Photochem. Photobiol. A: Chem.* **2002**, *154*, 81-92.

52. Mishra, A.; Krishnamoorthy, G. Photophysical Study of 2-(4′-*N,N*-dimethylaminophenyl)oxazolo[4,5-b]-pyridine in Different Solvents and at Various pH. *Photochem. Photobiol. Sci*. **2012**, *11*, 1356–1367.

53. Herbich, J.; Grabowski, Z. R.; Wo´jtowicz, H.; Golankiewicz, K. Dual Fluorescence of 4-(Dialkylamino)pyrimidines. Twisted Intramolecular Charge Transfer State Formation Favored-by Hydrogen Bond or by Coordination to the Metal Ion. *J. Phys. Chem*., **1989**, *93*, 3439–3444.

54. Birks, J.B., Photophysics of Aromatic Molecules, Wiley, New York, 1978.

55. Herbich, J.; Waluk, J. Excited Charge Transfer States in 4-Aminopyrimidines, 4-(Dimetylanilino)pyrimidine and 4-(Dimethylamino)pyridine. *Chem. Phys*. **1994**, *188*, 247–265.

56. Szydłowska, I.; Kyrychenko, A.; Nowacki, J.; Herbich, J. Photoinduced Intramolecular Electron Transfer in 4-Dimethylaminopyridines. *Phys. Chem. Chem. Phys*. **2003**, *3*, 1032–1038.

57. Szydłowska, I.F.; Nowacki, J.; Herbich, J., Structural Changes Accompanying Excited-state Electron Transfer in meta- and para-Dialkylaminopyridines, *J. Photochem. Photobiol. A* **2010,** *209*, 135–146.

58. Seo, J.; Kim, S.; Park, S. Y. Strong Solvatochromic Fluorescence From the Intramolecular Charge-Transfer State Created by Excited-State Intramolecular Proton Transfer. *J. Am. Chem. Soc*., **2004**, *126*, 11154–11155.

59. Kim, C. H.; Park, J.; Seo, J.; Park, S. Y.; Joo, T. Excited State Intramolecular Proton Transfer and Charge Transfer Dynamics of a 2-(2′-Hydroxyphenyl)benzoxazole Derivative in Solution, *J. Phys. Chem. A* **2010**, *114*, 5618–5629.

60. Balamurali M. M.; Dogra, S. K. Ground and Excited State Prototropism in 2-(2 '-methoxyphenyl)-*1H*-imidazo[4,5-c]pyridine. *J. Mol. Struct.* **2004**, *691*, 59-70.

61. Lippert, E. Spektroskopische Bistimmung Des Dipolmomentes Aromatischer Verbindugen Im Ersten Angeregten Singulettzustand. *Z. Electrochem.*, **1957**, *61*, 962–975.

62. Dash, N.; Krishnamoorthy G. Effect of Temperature on the Spectral Characteristics of 2-(4-N,N-dimethylaminophenyl)imidazo[4,5-b]pyridine. *Spectrochim. Acta A* **2012**, *95*, 540–546.

63. Kamlet, M. J.; Abboud, J. –L.; Abraham, M. H.; Taft, R. W. Linear Solvation Energy Relationships. 23. A Comprehensive Collection of the Solvatochromic Parameters, π*, α and β and Some Methods for Simplifying the Generalized Solvatochromic Equation. *J. Org. Chem.* **1983**, *48*, 2877-2887.

64. Frisch, M. J.; Trucks, G. W.; Schlegel, H. B.; Scuseria, G. E.; Robb, M. A.; Cheeseman, J. R.; Scalmani, G.; Barone, V.; Mennucci, B.; Petersson, G. A. *et al. Gaussian 09*, Revision D.01, Gaussian, Inc., Wallingford CT, 2013.

65. Kim, Y. H.; Cho, D. W.; Yoon, M.; Kim, D. Observation of Hydrogen-Bonding Effects on Twisted Intramolecular Charge Transfer of p-(*N*,*N*-Diethylamino)benzoic Acid in Aqueous Cyclodextrin Solutions. *J. Phys. Chem.*, **1996**, *100*, 15670–15676.

66. Kim, Y.; Lee, B. I.; Yoon, M. Excited-State Intramolecular Charge Transfer of *p-N,N*-Dimethylaminobenzoic acid in Y Zeolites: Hydrogen-Bonding Effects. *Chem. Phys. Lett.*, **1998**, *286*, 466–472.

Figure Captions

Chart 1. Structures of APIP-c, HPIP-c, AHPIP-c and AMPIP-c.

Chart 2: *Cis*-enol, *trans*-enol and keto forms of AHPIP-c.

Figure 1. Fluorescence spectra of APIP-c in (1) ethylacetate, (2) dioxane, (3) acetonitrile, (4) dimethylformamide, (5) 2-propanol, (6) butanol (7) methanol (λ_{exc} = 320 nm).

Figure 2. The instrument response function (a) and the fluorescence decays of APIP-c in propanol (b) λ_{em} = 380 nm and (c) λ_{em} = 460 nm along with fitted curve and residue plot (λ_{ecx} = 308 nm).

Figure 3. Fluorescence spectra of AHPIP-c in (1) ethylacetate, (2) acetonitrile, (3) 1-propanol, (4) butanol, (5) methanol, and (6) dimethyformamide (λ_{exc} = 340 nm).

Figure 4. Plot of tautomer band maximum against the dielectric constant of aprotic and protic solvents.

Figure 5. Fluorescence excitation spectra of AHPIP-c monitored at normal band maximum (dotted line) and tautomer band maximum (solid line) in methanol.

Figure 6. Plot of I_T/I_N Versus dielectric constant (ε).

Figure 7. Fluorescence spectra of AMPIP-c in (1) cyclohexane, (2) ethylacetate, (3) dioxane, (4) acetonitrile, (5) 1-propanol, and (6) methanol (λ_{exc} = 310 nm).

Figure 8. The instrument response function (a) and the fluorescence decays of AMPIP-c in methanol (b) along with fitted curve and residue plot (λ_{exc} = 308 nm and λ_{em} = 385 nm).

Figure 9. Lippert-Mataga plot using normal emission of APIP-c (●), AMPIP-c (■), and AHPIP-c (▲).

Figure 10. Fluorescence spectra of PIP-c in different solvents : (1) ether, (2) butanol, (3) 1-propanol, (4) ethanol, (5) methanol (λ_{exc} = 290 nm).

Figure 11. Frontier molecular orbitals (involved in the first excitation) of the amino twisted rotamer of APIP-c and AMPIP-c.

Table 1. Absorption Band Maxima (λ_{max}^{ab}, nm), Fluorescence Band Maxima (λ_{max}^{fl}, nm of APIP-c in Different Solvents

Solvent	λ_{max}^{ab}	λ_{max}^{fl}	
		Shorter Wavelength	Longer Wavelength
Methylcyclohexane		366, 394, 415	
Dioxane	309	367	
Ether	311	371	
Ethylacetate	310	369	
Tetrahydrofuran	313	375	
Acetonitrile	314	377	
Dimethylformamide	314	384	
Dimethylsulphoxide	317	385	
Butanol	316	383	
2-Propanol	316	384	
1-Propanol	318	383	
Ethanol	318	384	
Methanol	319	384	470

Table 2. Fluorescence Lifetime of APIP-c in Different Solvents Along With the Corresponding Chi Square (χ^2) Value (Values in the Parentheses are the Relative Amplitudes).

Solvent	λem = 380 nm		λem = 460 nm		
	τ	χ^2	τ_1	τ_2	χ^2
Dioxane	1.0	1.0			
Acetonitrile	1.2	1.0			
2-Propanol	1.3	1.0	1.1 (52.59)	2.7 (47.41)	1.0
Butanol	1.3	1.0	1.1 (46.34)	2.9 (53.66)	1.0
1-Propanol	1.3	1.0	1.0 (38.28)	2.8 (61.72)	1.0
Methanol	0.5	1.4	0.4 (27.43)	2.2 (72.57)	1.0

Table 3. Absorption Band Maxima (λ_{max}^{ab}, nm) and Fluorescence Band Maxima (λ_{max}^{fl}, nm) of AHPIP-c in Different Solvents

Solvent	λ_{max}^{ab}	λ_{max}^{fl}	
		Shorter Wavelength	Longer Wavelength
Methylcyclohexane	287, 327, 353	390, 420	474
Dioxane	296, 346	389	472
Ether		389	473
Ethylacetate	300, 346	388	465
Tetrahydrofuran	310, 347	388	464
Acetonitrile	297, 344	386	460
Dimethylformamide	300, 344	376	462
Dimethylsulphoxide	304, 443	379	462
Butanol	310, 346	384	455
2-Propanol	309, 346	382	451
1-Propanol	305, 345	389	452
Ethanol	307, 345	389	452
Methanol	303, 342	379	451

Table 4. Fluorescence Lifetime of Shorter Wavelength Emission (τ_S, ns) and Longer Wavelength Emission (τ_L, ns) of AHPIP-c in Different Solvents Along With The Corresponding Chi Square (χ^2) value

Solvents	τ_S	χ^2	τ_L	χ^2
Dioxane			3.0	1.0
Ethylacetate	1.2	1.0	3.9	1.2
Acetonitrile	1.2	1.1	3.1	1.0
Butanol	1.3	0.9	2.8	1.0
2-Propanol	1.4	1.0	3.2	1.0
1-Propanol	1.3	1.0	2.8	1.0
Ethanol	1.3	1.0	2.6	1.0
Methanol	1.1	1.0	2.3	1.0

Table 5. Absorption Band Maxima (λ_{max}^{ab}, nm) and Fluorescence Band Maxima (λ_{max}^{fl}, nm) of AMPIP-c in Different Solvents

Solvent	λ_{max}^{ab}	λ_{max}^{fl}	
		Shorter Wavelength	Longer Wavelength
Methylcyclohexane	297, 321, 334	339, 355, 374	
Cyclohexane	298, 320, 334	341, 356, 374	
Dioxane	300, 328	371	
Ether	301, 327	371	
Ethylacetate	302, 328	370	
Tetrahydrofuran	301, 328	373	
Acetonitrile	301, 329	373	
Dimethylformamide	302, 334	383	
Dimethylsulphoxide	304, 337	384	
Butanol	301, 336	381	
2-Propanol	301, 333	383	
1-Propanol	302, 336	383	
Ethanol	301, 336	383	
Methanol	302, 336	383	455

Table 6. Fluorescence Lifetime of AMPIP-c in Different Solvents Along With the Corresponding Chi Square (χ^2) Value, λem = 385 nm (Values in the Parentheses are the Relative Amplitudes).

Solvent	Single exponential decay		Biexponential decay		
	τ	χ^2	τ_1	τ_2	χ^2
Cyclohexane	1.1	0.9			
Dioxane	1.1	1.1			
Ether	1.2	1.0			
Ethylacetate	1.3	1.1			
Acetonitrile	1.3	1.1			
Butanol	1.4	1.1			
2-Propanol	1.4	1.0			
1-Propanol	1.4	1.1			
Ethanol	1.3	1.1			
Methanol	1.3	1.6	0.2 (82.72)	0.7 (17.28)	1.0

Table 7. Absorption Band Maxima (λ_{max}^{ab}, nm) and Fluorescence Band Maxima (λ_{max}^{fl}, nm) of PIP-c

Solvent	λ_{max}^{ab}	λ_{max}^{fl}
Cyclohexane	292, 311	316, 331, 345, 364
Ether	292, 309	317, 331, 346, 362
Butanol	291, 308	315, 329, 343, 361
2-Propanol	292, 308	315, 329, 343, 360
1-Propanol	291, 308	315, 329, 343, 361
Ethanol	290, 307	315, 329, 343, 361
Methanol	290, 307	315, 329, 344, 362

Table 8. The computed transitions, their energies (ΔE/eV) and the corresponding oscillator strengths (*f*) for APIP-c, AMPIP-c, and AHPIP-c in acetonitrile along with experimental (Exp) values.

Molecule	Transition		Excitation			Emission		
			ΔE	*f*	Exp[a]	ΔE	*f*	Exp
APIP-c	$S_0 \rightarrow S_1$	H→L	3.86	0.9732	3.95	3.56	1.1794	3.29
	$S_0 \rightarrow S_2$	(H→L+1), (H-2→L), (H→L+2)	4.47	0.0270		4.38	0.0260	
	$S_0 \rightarrow S_3$	(H→L+2), (H-4→L), (H-1→L), (H→L+1)	4.73	0.0488		4.57	0.0021	
AMPIP-c	$S_0 \rightarrow S_1$	(H→L)	4.07	0.7765	3.77	3.56	1.1604	3.32
	$S_0 \rightarrow S_2$	(H→L+1), (H→L+2), (H-2→L), (H-2→L+3)	4.60	0.0130		4.40	0.0037	
	$S_0 \rightarrow S_3$	(H→L+2), (H-4→L), (H-1→L)	4.87	0.0526		4.41	0.0081	
AHPIP-c	$S_0 \rightarrow S_1$	(H→L)	3.81	0.9314	3.70	3.02	0.3081	2.70
***cis*-enol/keto**[b]	$S_0 \rightarrow S_2$	(H-1→L), (H→L+1), (H→L+2), (H→L+3)	4.36	0.0157		3.64	0.0172	
	$S_0 \rightarrow S_3$	(H-2→L), (H-1→L), (H→L+1)	4.63	0.0488		3.83	0.6641	
AHPIP-c	$S_0 \rightarrow S_1$	(H→L)	3.89	0.9307	3.78	3.56	1.1008	3.21
***trans*-enol**	$S_0 \rightarrow S_2$	(H-2→L), (H-1→L), (H→L+2), (H→L+3)	4.53	0.0150		4.46	0.0363	
	$S_0 \rightarrow S_3$	(H→L+1) (H-4→L), (H-2→L), (H-1→L)	4.74	0.0494		4.60	0.0001	

[a]APIP-c and AMPIP-c from the absorption spectra and AHPIP-c from the excitation spectra. [b]Excitation cis-enol form and emission keto form. (H=HOMO and L=LUMO). The frontier molecular orbitals were presented in the Supporting Information.

Table 9. The computed transitions, their energies (ΔE/eV) and oscillator strengths (*f*) for different rotamers of APIP-c in methanol along with experimental (Exp) values.

Molecule	Transition		Excitation			Emission		
			ΔE	*f*	Exp	ΔE	*f*	Exp
Normal								
	$S_0 \rightarrow S_1$	H→L	3.90	0.9842	3.89	3.55	1.2110	3.23
	$S_0 \rightarrow S_2$	(H→L+1), (H→L+2),(H-1→L), (H-3→L)	4.52	0.0229		4.40	0.0186	
	$S_0 \rightarrow S_3$	(H→L+2), (H-1→L), (H-4→L), (H-3→L), (H→L+1)	4.72	0.0468		4.55	0.0027	
Phenyl twisted								
	$S_0 \rightarrow S_1$	(H→L)	4.25	0.0000		4.05	0.0000	
	$S_0 \rightarrow S_2$	(H→L+2),(H→L+1), (H-3→L+3)	4.80	0.0347		4.70	0.3626	
	$S_0 \rightarrow S_3$	(H→L+2),(H→L+1)	5.10	0.0026		4.81	0.0003	
Amino twisted								
	$S_0 \rightarrow S_1$	(H→L), (H→L+3)	3.73	0.0001		3.43	0.0000	2.64[a]
	$S_0 \rightarrow S_2$	(H-1→L)	4.28	0.8832		3.74	1.0143	
	$S_0 \rightarrow S_3$	(H-2→L), (H-4→L), (H-1→L+1), (H-1→L+2)	4.73	0.0142		4.49	0.0000	

(H=HOMO and L=LUMO). The frontier molecular orbitals were presented in the Supporting Information. [a]The error in the value is higher due to broadness and overlap.

Table 10. The computed transitions, their energies (ΔE/eV) and oscillator strengths (*f*) for different rotamers of AMPIP-c in methanol along with experimental (Exp) values.

Molecule	Transition		Excitation			Emission		
			ΔE	*f*	Exp	ΔE	*f*	Exp
Normal								
	$S_0 \rightarrow S_1$	(H→L)	3.91	0.7378	3.69	3.57	1.1460	3.24
	$S_0 \rightarrow S_2$	(H-1→L), (H-1→L+3), (H→L+1), (H→L+2)	4.54	0.0023		4.40	0.0323	
	$S_0 \rightarrow S_3$	(H→L+1), (H→L+2), (H-2→L), (H-1→L)	4.70	0.0972		4.54	0.0261	
Phenyl twisted								
	$S_0 \rightarrow S_1$	(H→L)	4.14	0.0001		3.88	0.0000	
	$S_0 \rightarrow S_2$	(H→L+1), (H→L+2), (H→L+3), (H-1→L+2), (H-1→L+3)	4.84	0.0874		4.68	0.3749	
	$S_0 \rightarrow S_3$	(H→L+1), (H→L+2), (H-1→L+1)	4.95	0.0001		4.71	0.0121	
Amino twisted								
	$S_0 \rightarrow S_1$	(H→L), (H→L+1), (H→L+3)	3.91	0.0002		3.55	0.0066	2.73[a]
	$S_0 \rightarrow S_2$	(H-1→L), (H-2→L)	4.44	0.6505		3.61	0.8901	
	$S_0 \rightarrow S_3$	(H-3→L), (H-3→L+2),(H-2→L), (H-1→L),(H-1→L+1), (H 1→L+1)	4.75	0.0792		4.30	0.1636	

(H=HOMO and L=LUMO). The frontier molecular orbitals were presented in Figure 11 and the Supporting Information. [a]As it not appears as clear band the error in the value is much higher.

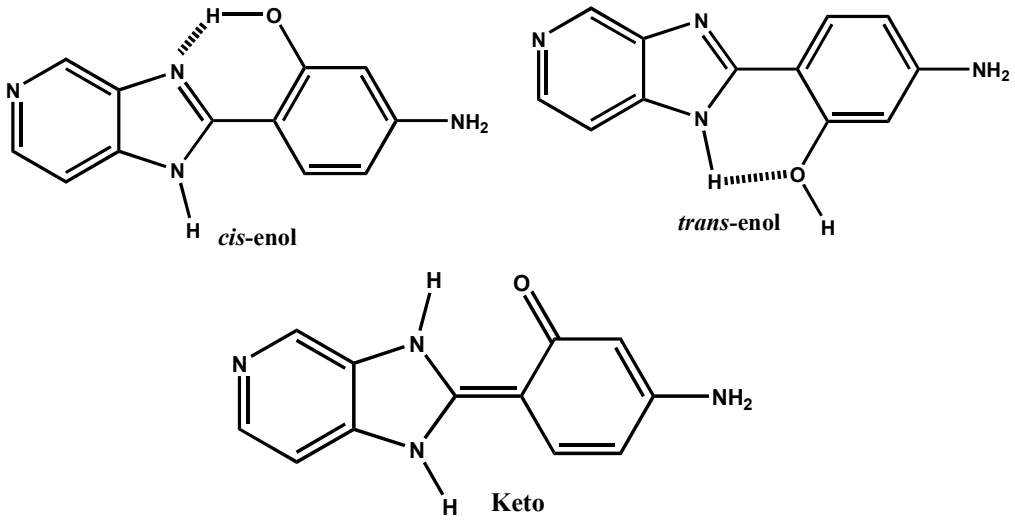

Chart 2: *Cis*-enol, *trans*-enol and keto forms of AHPIP-c.

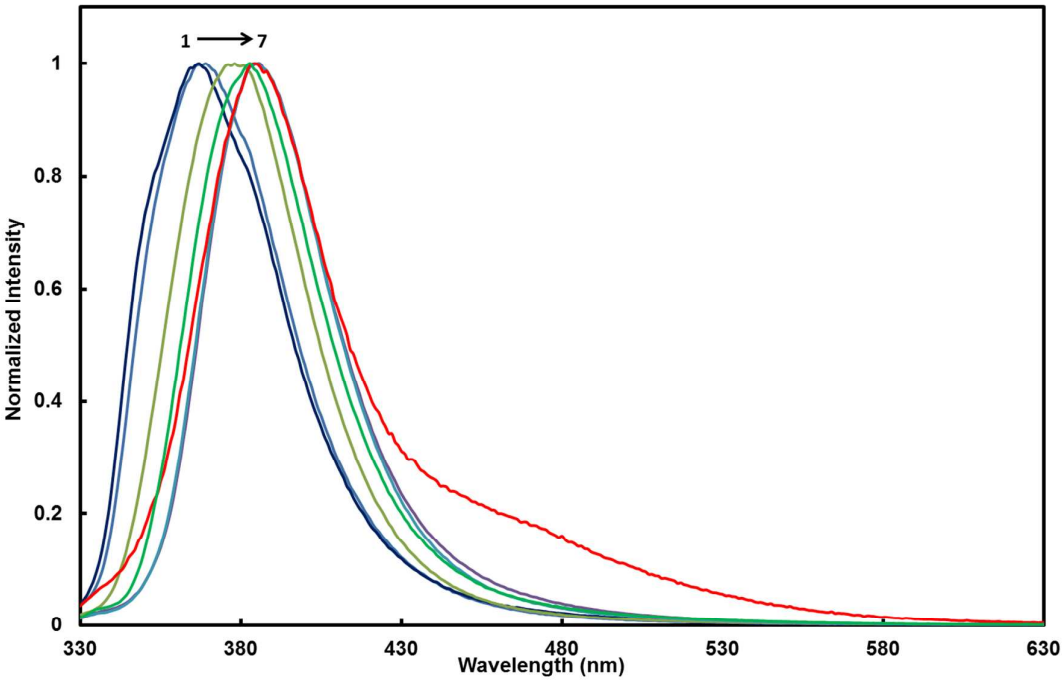

Figure 1. Fluorescence spectra of APIP-c in (1) ethylacetate, (2) dioxane, (3) acetonitrile, (4) dimethylformamide, (5) 2-propanol, (6) butanol (7) methanol (λ_{exc} = 320 nm).

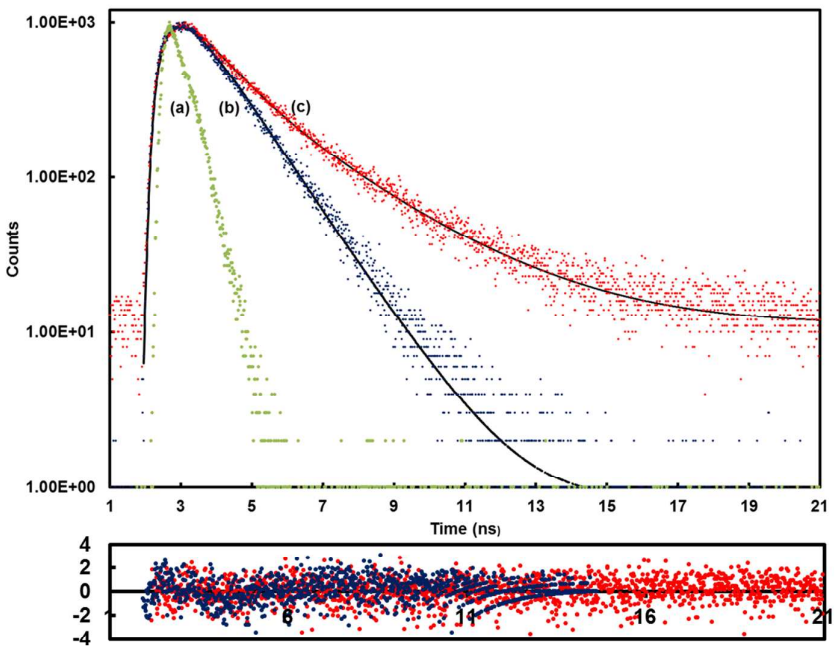

Figure 2. The instrument response function (a) and the fluorescence decays of APIP-c in propanol (b) λ_{em} = 380 nm and (c) λ_{em} = 460 nm along with fitted curve and residue plot (λ_{exc} = 308 nm).

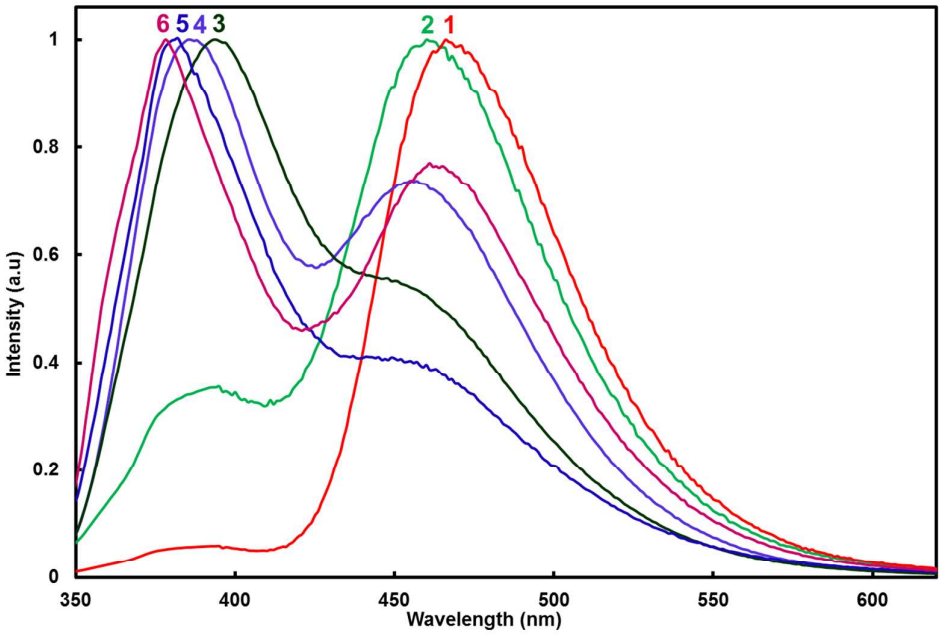

Figure 3. Fluorescence spectra of AHPIP-c in (1) ethylacetate, (2) acetonitrile, (3) 1-propanol, (4) butanol, (5) methanol, and (6) dimethyformamide (λ_{exc} = 340 nm).

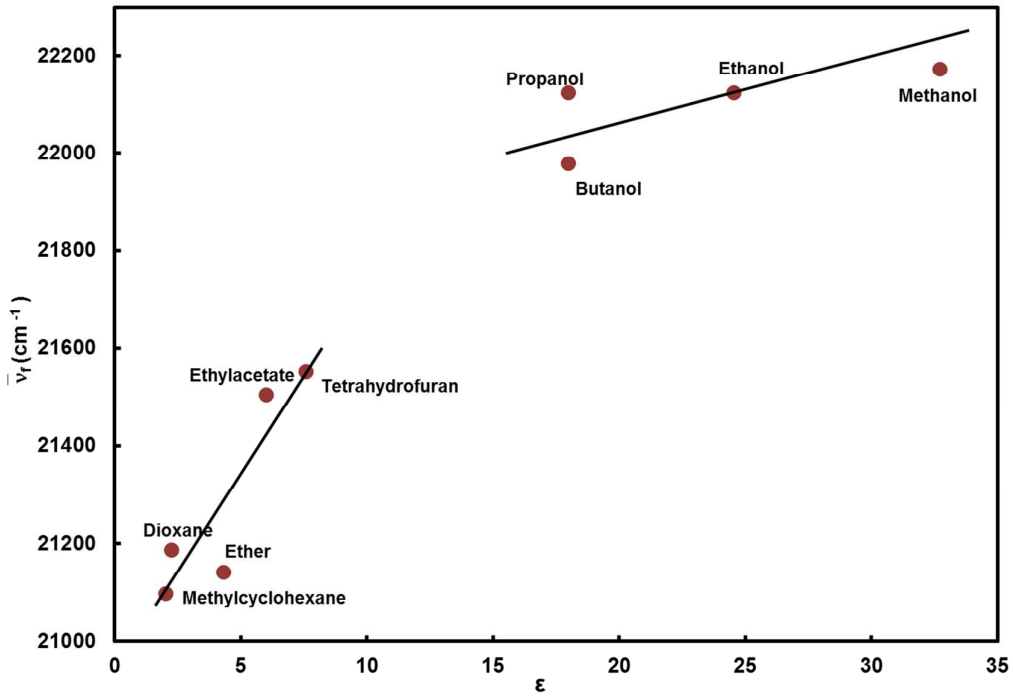

Figure 4. Plot of tautomer band maximum against the dielectric constant of aprotic and protic solvents.

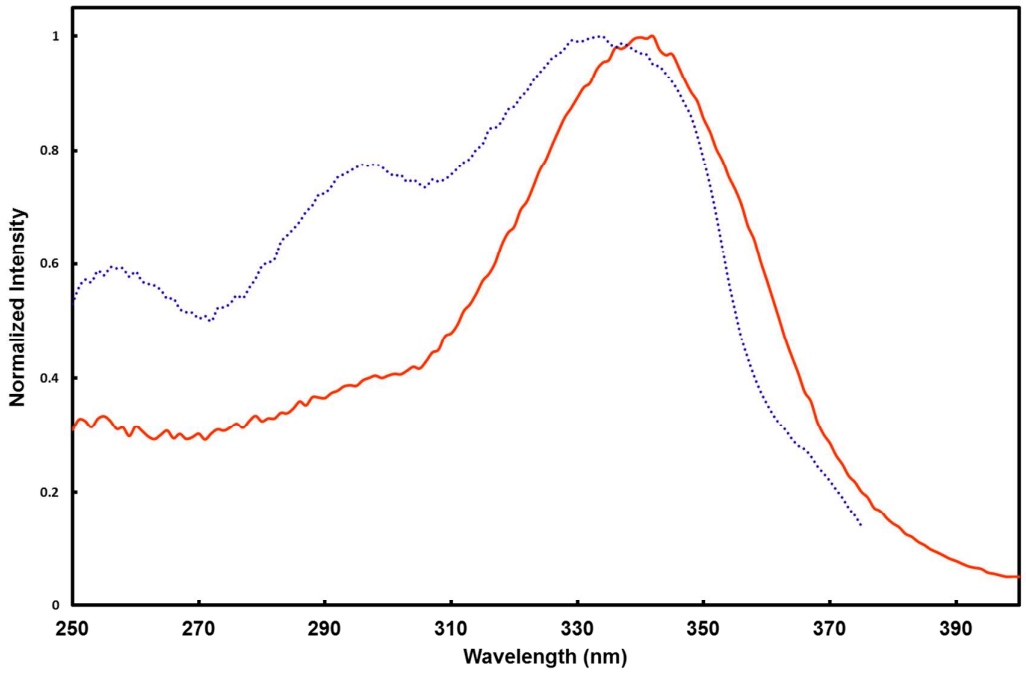

Figure 5. Fluorescence excitation spectra of AHPIP-c monitored at normal band maximum (dotted line) and tautomer band maximum (solid line) in methanol.

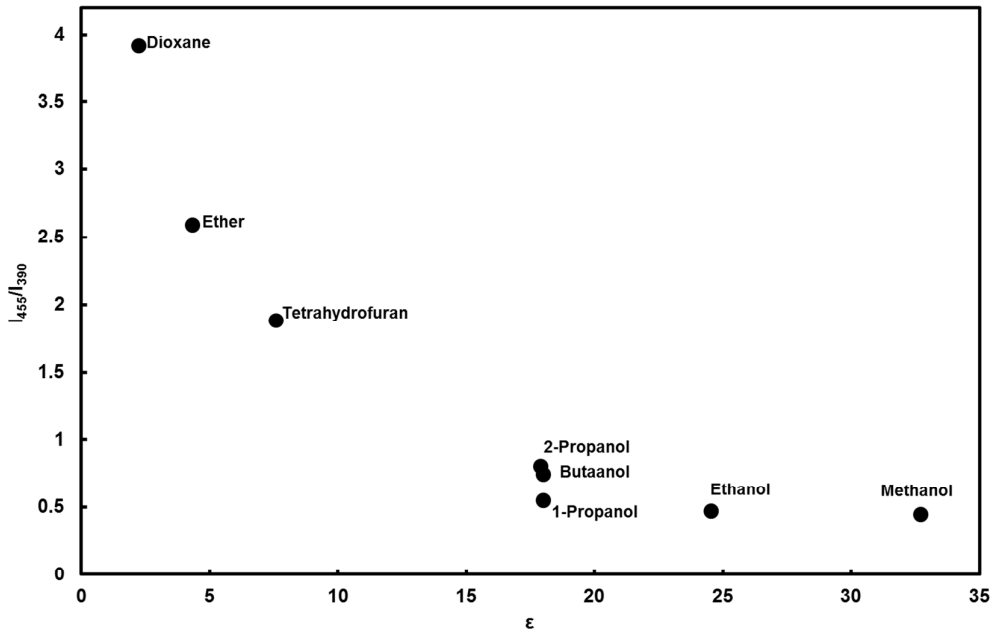

Figure 6. Plot of I_T/I_N Versus dielectric constant (ε).

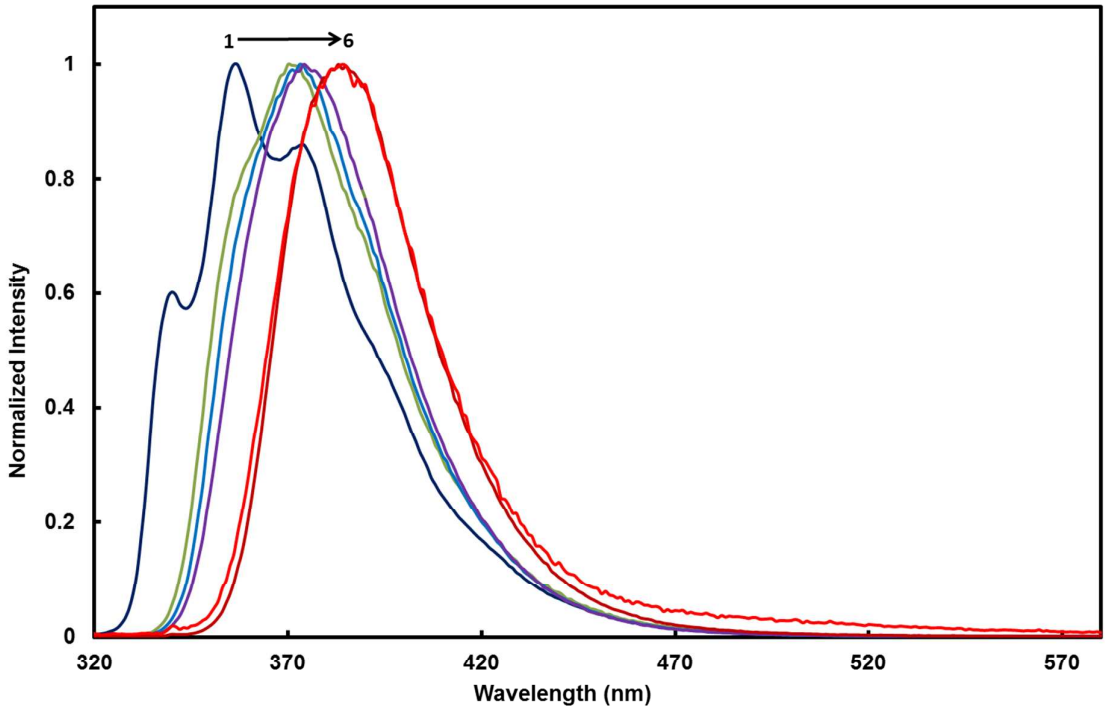

Figure 7. Fluorescence spectra of AMPIP-c in (1) cyclohexane, (2) ethylacetate, (3) dioxane, (4) acetonitrile, (5) 1-propanol, and (6) methanol (λ_{exc} = 310 nm).

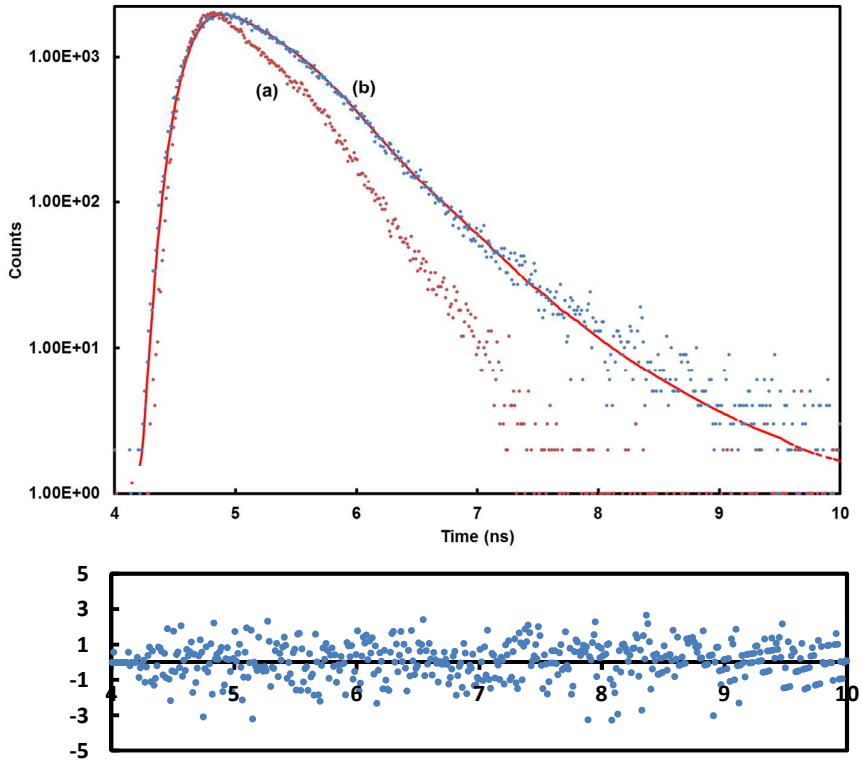

Figure 8. The instrument response function (a) and the fluorescence decays of AMPIP-c in methanol (b) along with fitted curve and residue plot, λ_{em} = 385 nm.

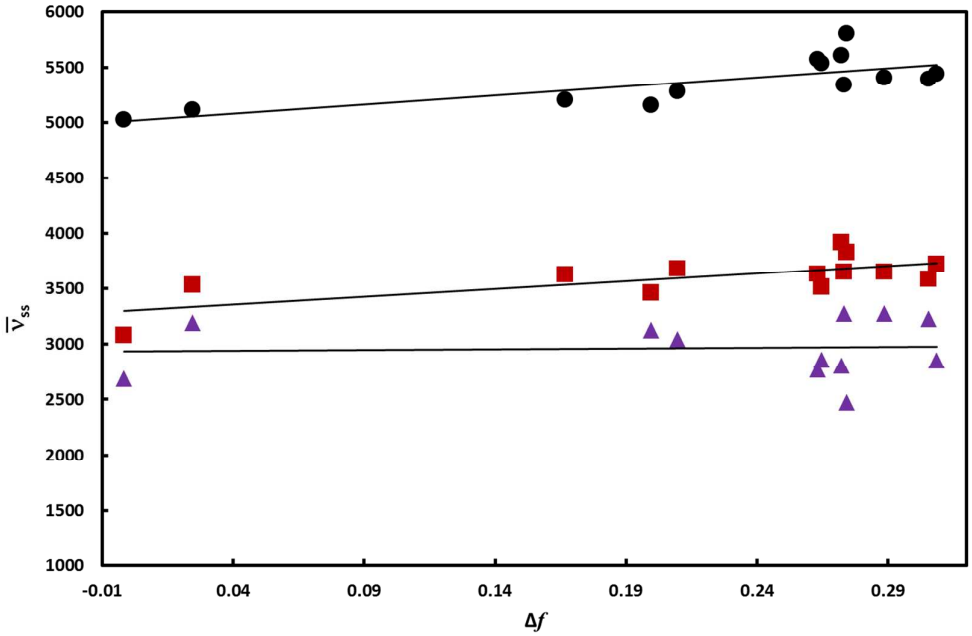

Figure 9. Lippert-Mataga plot using normal emission of APIP-c (●), AMPIP-c (■), and AHPIP-c (▲).

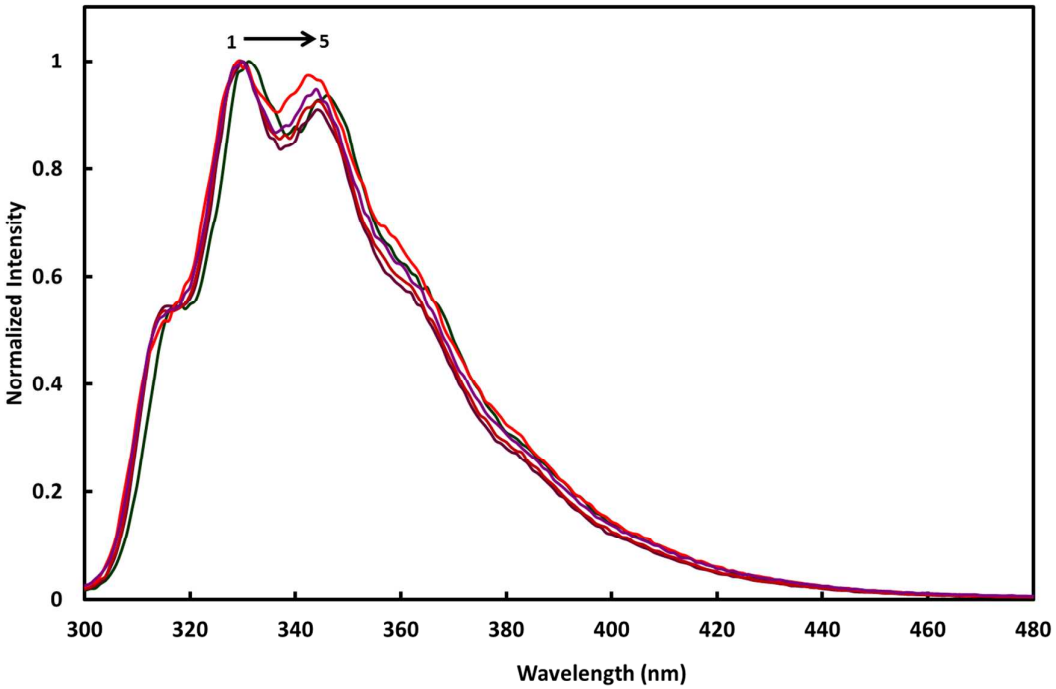

Figure 10. Fluorescence spectra of PIP-c in different solvents : (1) ether, (2) butanol, (3) 1-propanol, (4) ethanol, (5) methanol (λ_{exc} = 290 nm).

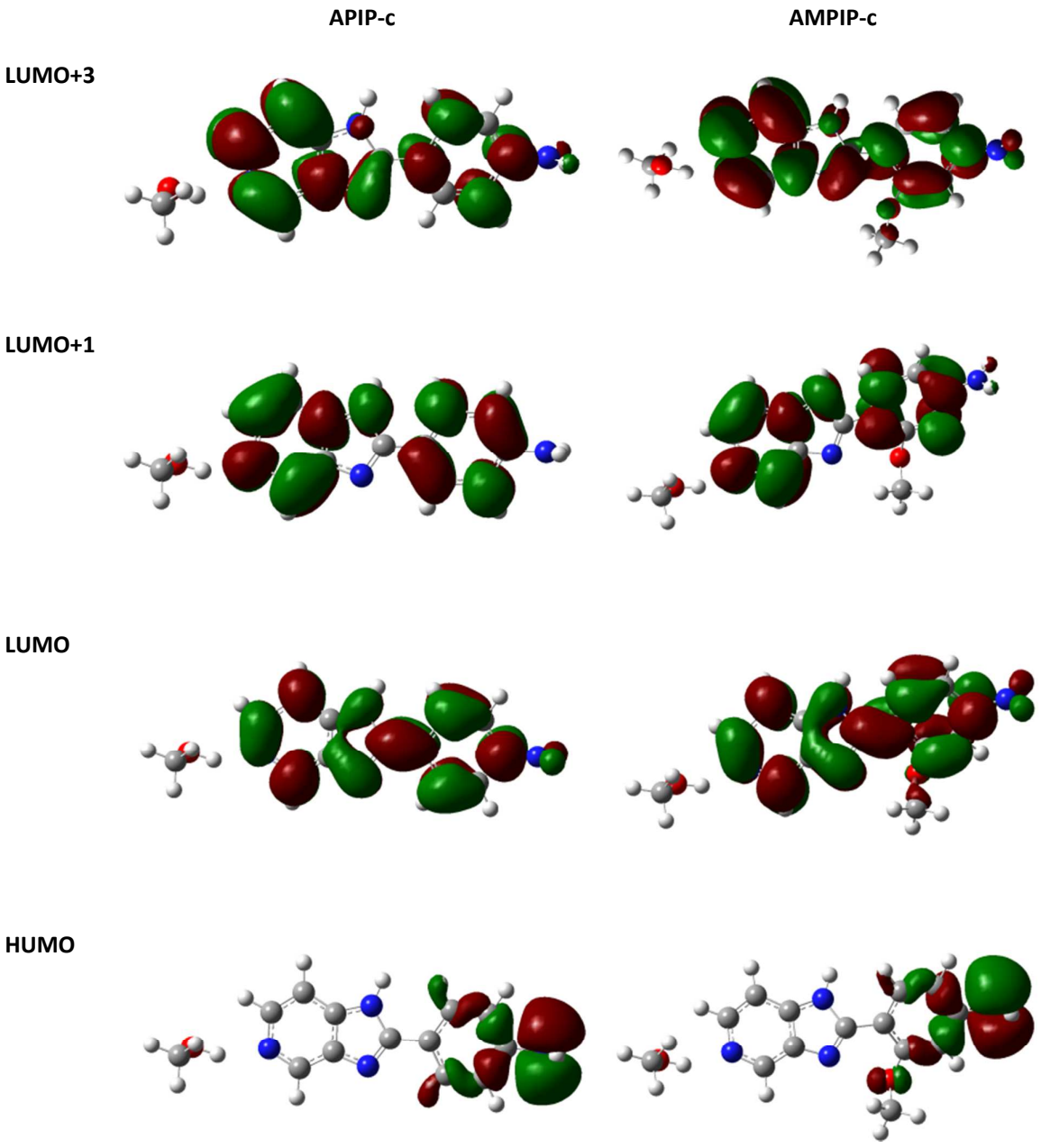

Figure 11. Frontier molecular orbitals (involved in the first excitation) of the amino twisted rotamer of APIP-c and AMPIP-c.

Table of Content Image